Static properties of a warm dense uniform electron gas

Cite as: Phys. Plasmas **28**, 112704 (2021); https://doi.org/10.1063/5.0062259
Submitted: 03 July 2021 • Accepted: 24 October 2021 • Published Online: 17 November 2021

J. Ara, Ll. Coloma and I. M. Tkachenko

Physics of Plasmas ARTICLE scitation.org/journal/php

Static properties of a warm dense uniform electron gas

Cite as: Phys. Plasmas **28**, 112704 (2021); doi: 10.1063/5.0062259
Submitted: 3 July 2021 · Accepted: 24 October 2021 ·
Published Online: 17 November 2021

J. Ara,[1] Ll. Coloma,[2] and I. M. Tkachenko[3,a)]

AFFILIATIONS

[1]Instituto de Tecnología Química, Universitat Politècnica de València-Consejo Superior de Investigaciones Científicas, Camino de Vera s/n, 46022 Valencia, Spain
[2]Departamento de Ingeniería Química y Nuclear, Universitat Politècnica de València, Camino de Vera s/n, 46022 Valencia, Spain
[3]Departament de Matemàtica Aplicada, Universitat Politècnica de València, Camino de Vera s/n, 46022 Valencia, Spain

[a)]**Author to whom correspondence should be addressed:** imtk@mat.upv.es; **Also at:** Al-Farabi Kazakh National University, al-Farabi Av. 71, 050040 Almaty, Kazakhstan

ABSTRACT

We show how the static dielectric function and other static characteristics of dense warm charged Fermi liquids can be obtained exclusively from the system static structure factor. The non-perturbative self-consistent method of moments is employed to extend onto quantum fluids, a similar reduction stemming from the fluctuation-dissipation theorem and other exact relations for classical one-component plasmas. The results are compared to and complement the numerical data obtained recently by the path-integral Monte Carlo method. Alternative theoretical approaches are discussed and employed as well.

I. INTRODUCTION

Contemporary numerical methods of investigation of the properties, both static and dynamic, of strongly coupled plasmas and warm dense matter, in particular, Ref. 1 are, certainly, very fruitful, especially, when real experiments are rare and seldom admit simple interpretation. Such an interpretation cannot avoid using model considerations. Indeed, to mention a few examples that are the most known and useful for the purpose of the present work: the Kohn–Sham density functional theory (KS DFT)[2–4] and the faster orbital-free DFT[5] are based on the Thomas–Fermi model, while molecular dynamics (MD) and the quantum-mechanical MD methods need a model effective potential and the DFT input. Even most advanced path-integral Monte Carlo (PIMC) methods[1,6,7] using contemporary neural-network/learning developments[8] while being, in principle, exact are limited to a wavenumber range $k > 2\pi/L$ (with L being the box length) and, therefore, have to be combined, e.g., with the STLS model,[9,10] etc.

Theoretical approaches are basically model ones, but they permit for an insight, which might be unavailable in numerical studies and can clarify the dependence of the properties under scrutiny on the physical and model parameters. This is why we present here a theoretical description of recently achieved *ab initio* PIMC data on the static properties of a dense warm uniform electron gas (UEG), which is a one-component normal quantum liquid of charged fermions.[11] Our aim is to express the static dielectric function and other static characteristics of such a Fermi liquid in terms of the system static structure factor (SSF). This connection is well-known for classical fluids as it stems from the fluctuation-dissipation theorem. For quantum liquids, we present two versions of this relation, without and with the energy dissipation processes taken into account. Our analysis is based on sum rules and other exact properties so that the above reduction relations are effectively interconnections between two different sum rules. The mathematical nature and the robustness of the proposed approach permit one to show that under the warm-dense-matter conditions, the obtained relations produce results that are in agreement with the PIMC data even when instead of using the proper static structure factor, we employ two different SSF fittings formally valid for classical one-component Coulomb systems only. We deal here with a weakly coupled quantum fluid so that it is not surprising that the standard random-phase approximation (RPA) provides consistent results for its static characteristics as well. The systems we consider are presumed to be in thermal equilibrium.

One cannot effectively separate the static properties of a Coulomb system from its dynamic characteristics. On the other hand, if we wish to study the dynamic properties of a dense warm electron gas, we think in the first place of the quasi-localized charge approximation (QLCA)[12] and the memory-function model.[13,14] As it is well known,[15] either not all of available sum rules are taken into account in these approaches or to satisfy the coupling-related sum rule, some

adjustment to the simulation data are required. This is not the case if one applies the moment approach, specifically, its self-consistent version complemented by physical considerations.[16–18] Like the QLCA, this approach connects the static structural correlation properties of quantum liquids of charged fermions to their dynamic, time dependent collective behavior, but unlike the QLCA, it does it with the account of the energy dissipation effects. This is another reason for the detailed analysis of the static properties of quantum Coulomb liquids carried out in this work. This analysis includes several alternative approaches, in particular, the one based on the random-phase approximation and the RPA improved by a static local-field correction.

In a finite-temperature one-component charged Fermi liquid, the density-density dynamic structure factor (DSF)

$$S(k,\omega) = \int_{-\infty}^{\infty} \langle \rho(\mathbf{k},t)\rho(-\mathbf{k},0)\rangle \exp(i\omega t)dt, \tag{1}$$

with the expectation value $\langle \cdots \rangle$ calculated with respect to the unperturbed Hamiltonian is the spectral density of the system longitudinal inverse dielectric function only in the limiting case of classical statistics. Otherwise, a model for the DSF is needed to determine the static dielectric function and other static characteristics like the static response function. Such a DSF model can be constructed in the random-phase or the extended random-phase approximation using an adequate local-field correction function or within some memory-function models. These approaches are perfectly valid in the low-density collisionless systems but begin to fail as the system density increases and/or the system temperature is of the order of its Fermi temperature. In the present work, we show how the self-consistent version of the method of moments applied in Refs. 16–18 to classical one-component plasmas can be extended to obtain a quantitative agreement with the PIMC data of Refs. 1 and 7. Since in dense warm or strongly coupled Fermi liquids, all characteristic lengths are of the same order,[1] such systems possess no small parameters, and the non-perturbative moment approach to the description of their properties is especially adequate. Within the moment approach, first five DSF sum rules are satisfied automatically, and these sum rules can be calculated from the system static structure factor independently and exactly.

This paper is organized in the following way. In Secs. II and III, we define the parameters and characteristics we study here, introduce the sum rules, and provide mathematical and physical aspects of the moment method background taking into account physical properties like the energy dissipation. The model based on the extended random-phase approximation is then outlined along with two alternative fitting methods involving the hyper-netted chain approximation. All these approaches are then applied to determine the electron gas static characteristics, which are the static structure factor

$$S(k) = \frac{1}{n}\int_{-\infty}^{\infty} S(k,\omega)d\omega = 1 + n\int (g(r)-1)\exp(-i\mathbf{k}\cdot\mathbf{r})d\mathbf{r} \tag{2}$$

(n being the number density of charged particles), the zero-distance value of the radial distribution function, $g(0)$, the static dielectric function, and the screened susceptibility. The last two characteristics are evaluated with and without accounting for the energy dissipation. Our numerical results are further compared to available recent numerical data obtained using the path-integral Monte Carlo method, and the energy dissipation is shown to be necessary to obtain a qualitative agreement with the PIMC data. It is somewhat surprising that this level of agreement is achieved even using the classical fittings for the SSF. This paper is concluded with a discussion of the obtained results and the perspectives we envisage, in particular, with respect to the new PIMC dynamic data,[20,21] see also Refs. 22 and 23. Additional mathematical details are given in the supplementary material.

II. PARAMETERS AND SUM RULES

As we have mentioned, the non-perturbative method of moments is especially auspicious when there are no small parameters in systems whose properties we wish to describe. We refer to the standard coupling and degeneracy parameters defined, respectively, as

$$\Gamma = \beta e^2/a\,, \quad D = \beta E_F = \theta^{-1}\,, \quad r_s = a/a_B, \tag{3}$$

in a strongly coupled Coulomb system they span two or even three orders of magnitude so that all characteristic lengths in these systems are comparable and vary around 1Å.[26] Here, a, a_B, E_F, and $n = 3/4\pi a^3$ are the Wigner–Seitz and Bohr radii, the Fermi energy, and the number density of charged particles (electrons), respectively; besides, the temperature $T = (k_B\beta)^{-1}$, and

$$r_s = \frac{\Gamma\theta}{2}\left(\frac{9\pi}{4}\right)^{\frac{2}{3}} = 1.842\Gamma\theta\,.$$

In warm dense matter,[1] the dimensionless parameters r_s, and θ vary around 1, and in the present work, we consider this the realm of their variation. Nevertheless, the approach we suggest is non-perturbative so that the region of parameter values can be extended as soon as new simulation data appear. Throughout the text, we use the dimensionless wavenumber q = ka.

A. The dielectric and loss functions

Modeling of the dielectric function $\varepsilon(q,\omega)$ or the inverse dielectric function $\varepsilon^{-1}(q,\omega)$ (the genuine response function[15,27,28]) of Coulomb fluids is actively discussed in the literature[29] nowadays. The loss function associated with the inverse dielectric function,

$$\mathscr{L}(q,\omega) = -\mathrm{Im}\varepsilon^{-1}(q,\omega)/\omega \geq 0, \tag{4}$$

determines the polarizational stopping power of such systems,[30] the reflectivity of shock-compressed plasmas,[31,32] etc. By virtue of the fluctuation-dissipation theorem, the loss function is related to the dynamic structure factor

$$S(q,\omega) = \frac{q^2 n}{3\pi\Gamma}B(\beta\hbar\omega)\mathbf{L}(q,\omega)\,. \tag{5}$$

Notice that

$$B(x) = x(1-\exp(-x))^{-1} \underset{x\to 0}{\simeq} 1. \tag{6}$$

In addition to the requirements of the loss function non-negativity for $\forall\omega \in \mathbb{R}$, and the analyticity of the prolongation of the inverse dielectric function onto the upper half-plane of complex frequency $\mathrm{Im}(\omega + i\delta) > 0$. The dielectric function analyticity might breakdown if the static dielectric function, $\varepsilon(q,0)$, becomes negative, see Ref. 27 and references therein. The models of $\varepsilon^{-1}(q,\omega)$ must be conditioned by the sum rules (which are effectively additional conservation laws),

and other exact relations.[33] Only if all these conditions are satisfied, the strongly or moderately coupled plasma dispersion relation and other dynamic properties can be studied in a consistent way.

The long way to the current situation with the inverse dielectric function of a liquid of charged fermions was initiated by Lindhard.[30] This collisionless (ideal) system model was generalized by Mermin[34] and later by Das[35] to take the collisions into account in the relaxation-time approximation. Mathematical properties of the Lindhard dielectric function were further studied in a number of elaborate publications, see, e.g., Ref. 36. The dielectric function in the random-phase approximation and at a non-zero temperature was found in the seminal papers by Khana and Glyde[37] and by Gouedard and Deutsch;[38] Arista and Brandt[39] managed to rewrite the RPA dielectric function in a more suitable for calculations way. The asymptotic behavior of the RPA dielectric function was studied in Refs. 38 and 39 in detail. These and other models of the inverse dielectric function were tested against the sum rules in Ref. 40. The random-phase approximation for the dielectric function was improved by taking into account static and dynamic local-field corrections.[41–54] The STLS model with the static local-field correction[9,10] is still considered to be a useful tool, in particular, at small wavenumbers,[1] though the employment of the static local-field correction leads to the violation of the coupling-related sum rule.[40]

B. The frequency power moments

The sum rules can be introduced as the loss function frequency power moments

$$C_\nu(q) = \frac{1}{\pi}\int_{-\infty}^{\infty} \omega^\nu \mathscr{L}(q,\omega)d\omega, \quad \nu = 0, 2, 4. \tag{7}$$

Notice that the odd-order moments vanish due to the symmetry of the loss function. It is also easy to observe[15,27] that by virtue of the fluctuation-dissipation theorem (5) and the detailed balance condition

$$S(q,-\omega) = \exp(-\beta\hbar\omega)S(q,\omega),$$

we have a direct relation between the moments (7) and the often employed power moments of the dynamic structure factor

$$C_\nu(q) = \frac{3e^2}{aq^2\hbar}\left[1+(-1)^\nu\right]\langle\omega^{\nu-1}\rangle, \quad \nu = 0, 1, 2, 3, 4,$$

where

$$\langle\omega^\ell\rangle = \frac{1}{n}\int_{-\infty}^{\infty}\omega^\ell S(q,\omega)d\omega, \quad \ell = -1, 0, 1, 3.$$

The sum rules or the moments $C_0(q)$, C_2, $C_4(q)$ and the characteristic frequencies,

$$\omega_1(q) = \sqrt{C_2/C_0(q)} \tag{8}$$

and

$$\omega_2(q) = \sqrt{C_4(q)/C_2}, \tag{9}$$

are known independently, they are determined by the system composition, degeneracy, and thermodynamics in terms of the moment

$$\langle\omega^0\rangle = \frac{1}{n}\int_{-\infty}^{\infty} S(q,\omega)d\omega = S(q) \tag{10}$$

and do not depend on the dielectric function model involved. Indeed, it immediately stems from the Kramers–Kronig relations for the inverse dielectric function that

$$C_0(q) = 1 - \varepsilon^{-1}(q,0), \tag{11}$$

while the moment

$$C_2 = \omega_p^2 \tag{12}$$

(ω_p being the plasma frequency) is the f-sum rule; the loss function fourth power moment for the electron gas, which is a particular case of one-component plasmas (OCPs), was found by Kugler[55] and Pathak and Vashishta,[56] and earlier in Ref. 57, see also Refs. 58 and 59,

$$C_4(q) = \omega_p^4\left[1 + K(q) + U(q)\right], \tag{13}$$

$$K(q) = \frac{q^2}{\Gamma}\theta^{3/2}F_{3/2}(\eta) + \frac{q^4}{12r_s}, \tag{14}$$

$$U(q) = \frac{1}{3\pi}\int_0^\infty \left[S(p)-1\right]f(p,q)p^2dp, \tag{15}$$

where

$$f(p,q) = \frac{5}{6} - \frac{p^2}{2q^2} + \frac{\left(p^2-q^2\right)^2}{4q^3p}\ln\left|\frac{q+p}{q-p}\right|. \tag{16}$$

Here,

$$F_\mu(\eta) = \int_0^\infty \frac{x^\mu}{\exp(x-\eta)+1}dx$$

is the order-μ Fermi integral, and η is the system dimensionless chemical potential determined by the normalization condition $F_{1/2}(\eta) = 2/(3\theta^{3/2})$. For multicomponent plasmas, these moments were obtained in Refs. 60 and 61.

As it was said, in the present work, we obtain a direct relation between the characteristic frequencies (8) and, thus, relate the zero moment $C_0(q)$ and the static dielectric function $\varepsilon(q,0)$ to the system static structure factor. The latter also defines the fourth frequency moment, and it is much easier to calculate; there is a number of corresponding methods, e.g., the hyper-netted chain approach and its modern modifications, see Refs. 62 and 63, and the molecular dynamics and Monte Carlo simulations including their quantum-mechanical versions.[7]

III. CANONICAL AND NON-CANONICAL SOLUTIONS OF THE TRUNCATED HAMBURGER MOMENT PROBLEM

The truncated classical Hamburger problem of moments[64,65] consists in the reconstruction of a non-negative function $M(\omega)$ defined on the whole real axis by the values of a finite number of its power moments

$$\mu_\ell = \int_{-\infty}^{\infty}\omega^\ell M(\omega)d\omega, \quad \ell = 0, 1, 2, \ldots 2\upsilon, \quad \upsilon = 0, 1, 2, \ldots. \tag{17}$$

This problem is solvable if and only if the sequence of the moments $\{\mu_0, \mu_1, \ldots, \mu_{2\upsilon}\}$ is positive-definite, i.e., if

$$\mu_0 > 0, \quad \det\begin{pmatrix} \mu_0 & \mu_1 \\ \mu_1 & \mu_2 \end{pmatrix} \geq 0, \ldots,$$
$$\det\begin{pmatrix} \mu_0 & \mu_1 & \cdots & \mu_\upsilon \\ \mu_1 & \mu_2 & \cdots & \mu_{\upsilon+1} \\ \vdots & \vdots & \ddots & \vdots \\ \mu_\upsilon & \cdots & \cdots & \mu_{2\upsilon} \end{pmatrix} \geq 0. \tag{18}$$

It is obvious that a solvable truncated moment problem can possess only an infinite number of solutions. Unique solutions occur only in some specific cases[65] hardly corresponding to real physical systems, except for the Gauss distribution density possessing unique properties.[66]

A. Canonical solutions

To satisfy the moment conditions (17), one can consider a singular density

$$M(\omega) = \sum_{\ell=0}^{2\upsilon} \rho_\ell \delta(\omega - \xi_\ell), \tag{19}$$

which actually consists of $2\upsilon + 1$ point "masses" located at some distinct points of the real axis, $\{\xi_\ell\}_{\ell=0}^{2\upsilon}$. These are the *canonical solutions* of the problem. The solution presentation (19) can be substituted into the conditions (17), and the "masses" $\{\rho_\ell\}_{\ell=0}^{2\upsilon}$ can be obtained directly from the linear algebraic system with the determinant, which is the non-zero Van der Monde determinant of an arbitrary set of distinct numbers $\{\xi_\ell\}_{\ell=0}^{2\upsilon}$

$$\begin{pmatrix} 1 & 1 & \cdots & 1 \\ \xi_0 & \xi_1 & \cdots & \xi_{2\upsilon} \\ \vdots & \vdots & \ddots & \vdots \\ \xi_0^{2\upsilon} & \xi_1^{2\upsilon} & \cdots & \xi_{2\upsilon}^{2\upsilon} \end{pmatrix} \begin{pmatrix} \rho_0 \\ \rho_1 \\ \vdots \\ \rho_{2\upsilon} \end{pmatrix} = \begin{pmatrix} \mu_0 \\ \mu_1 \\ \vdots \\ \mu_{2\upsilon} \end{pmatrix}. \tag{20}$$

In other words, we obtain an infinite number of canonical solutions parametrized by the latter set of points of the real axis.

In our context, the density we consider is

$$M(\omega) = \frac{1}{\pi} \mathscr{L}(q, \omega), \tag{21}$$

so that the moments

$$\mu_\nu = C_\nu(q), \quad \nu = 0, 1, 2, 3, 4,$$

and in this five-moment approximation ($\upsilon = 2$), one can choose five location points as $\{\xi_\ell\}_{\ell=0}^{4} = \{0, \pm\omega_1(q), \pm\omega_2(q)\}$ and then the solution of Eq. (20) implies that[67]

$$\mathscr{L}_2^{\text{can}}(q, \omega) = \pi C_0(q) \left[\left(1 - \frac{\omega_1^2(q)}{\omega_2^2(q)}\right)\delta(\omega) + \frac{\omega_1^2(q)}{\omega_2^2(q)}\delta\left(\omega^2 - \omega_2^2(q)\right)\right], \tag{22}$$

i.e., there is no contribution related to the frequency $\omega_1(q)$. The corresponding dynamic structure factor model,

$$S_2(q, \omega) = \frac{q^2 n}{3\pi\Gamma} B(\beta\hbar\omega) \mathscr{L}_2^{\text{can}}(q, \omega), \tag{23}$$

is a physically plausible result: the dynamic structure factor has at most three extrema at the frequencies $\omega = 0$ and $\omega = \pm\omega_2(q)$. By integration of this last expression, we immediately obtain that

$$q^2 C_0(q) \left(1 - \frac{\omega_1^2}{\omega_2^2}\left(1 - \frac{\beta\hbar\omega_2}{2}\coth\left(\frac{\beta\hbar\omega_2}{2}\right)\right)\right) = 3\Gamma S(q),$$

and that

$$\omega_1^2(q) = \frac{\omega_2^2(q)}{1 + \dfrac{3\Gamma\omega_2^2(q)}{q^2\omega_p^2} S(q) - \dfrac{\beta\hbar\omega_2(q)}{2}\coth\dfrac{\beta\hbar\omega_2(q)}{2}}. \tag{24}$$

Certainly, the classical limiting form of Eq. (24),

$$\omega_1^2 \underset{\hbar\to 0}{\simeq} \frac{\omega_p^2 q^2}{3\Gamma S(q)} + \left[\frac{\beta\hbar\omega_p^2 q^2}{6\sqrt{3\Gamma S(q)}}\right]^2 + O(\hbar^4), \tag{25}$$

follows also from the classical version of the fluctuation-dissipation theorem (5). In classical systems like the classical one-component plasmas, it connects the static dielectric function to the static structure factor. Now, by virtue of Eqs. (11) and (8), we obtain from Eq. (24) an expression for the (inverse) static dielectric function valid in both one-and multi-component quantum systems

$$\varepsilon^{-1}(q, 0) = 1 - \frac{3\Gamma}{q^2} S(q) - \frac{\omega_p^2}{\omega_2^2} + \frac{\beta\hbar\omega_p^2}{2\omega_2}\coth\frac{\beta\hbar\omega_2}{2}, \tag{26}$$

where the fourth moment [(9) and (13)] plays an important role. In a classical weakly coupled system (26) satisfies the Debye model

$$\varepsilon(q, 0) \underset{\hbar\to 0}{\simeq} \frac{q^2}{q^2 - q_D^2 S(q)}, \quad q_D^2 = 3\Gamma,$$

like in the three-moment case, see Ref. 18. A detailed comparative study of Eq. (26), in particular, at very low temperatures, is to be carried out elsewhere.

We can also observe that due to the ideal screening condition[11] $\lim_{q\to 0} \varepsilon^{-1}(q) = 0$ and the definitions [(11) and (8)] $\omega_1(q \to 0) \simeq \omega_p$. By virtue of the definitions [(9) and (13)] in a quantum liquid, we have also that $\omega_2(q \to 0) \simeq \omega_p$. Thus, we recover a well-known long-wavelength limiting form of the static structure factor valid at any temperature[48]

$$S(q \to 0) \simeq \frac{\hbar q^2}{2a^2 m\omega_p}\coth\frac{\beta\hbar\omega_p}{2}.$$

We can rewrite (23) as

$$\frac{S_2(q,\omega)}{nS(q)} = \frac{\left(1-\frac{\omega_1^2(q)}{\omega_2^2(q)}\right)\delta(\omega) + \frac{\beta\hbar\omega_1^2(q)}{2\omega_2(q)}\left(\frac{\delta(\omega-\omega_2(q))}{1-\exp\left(-\beta\hbar\omega_2(q)\right)} - \frac{\delta(\omega+\omega_2(q))}{1-\exp\left(\beta\hbar\omega_2(q)\right)}\right)}{1-\frac{\omega_1^2}{\omega_2^2}\left(1-\frac{\beta\hbar\omega_2}{2}\coth\left(\frac{\beta\hbar\omega_2}{2}\right)\right)} \tag{27}$$

and observe that when $\beta \to \infty$, we return to the Feynman classical asymptotic form[68]

$$S_2(q,\omega) = nS(q)\delta(\omega-\omega_2(q))$$

and notice that at zero temperature, the system may only absorb energy.

B. Non-canonical solutions

On the other hand, and if we look for at least continuous solutions of the Hamburger moment problem, we can employ Nevanlinna's linear fractional transformation (theorem)[64,69,70]

$$\int_{-\infty}^{\infty}\frac{M(\omega)d\omega}{z-\omega} = \frac{E_{\upsilon+1}(z)+R_\upsilon(z)E_\upsilon(z)}{D_{\upsilon+1}(z)+R_\upsilon(z)D_\upsilon(z)}, \tag{28}$$

which provides a bijection between the *non-canonical* solutions of the Hamburger problem and the Nevanlinna parameter functions (NPFs), $R_\upsilon(z=\omega+i\delta)$. Any NPF, exactly like any response (Nevanlinna) function, must be analytic and possess a non-negative imaginary part in the upper half-plane $\delta > 0$, being at least continuous on its closure $\delta = 0$. In addition, the NPF must (uniformly within any angle $\vartheta \le \arg(z) \le \pi-\vartheta, 0<\vartheta<\pi$) satisfy the following limiting condition:

$$\lim_{z\to\infty}\frac{R_\upsilon(z)}{z} = 0. \tag{29}$$

This important property of the NPF guarantees the automatic satisfaction, by the density $M(\omega)$, of the involved sum rules. The coefficients of the one-to-one transformation $M(\omega) \leftrightarrow R_\upsilon(z)$, Eq. (28), are real orthogonal polynomials with the weight $M(\omega)$,[40,64,70] which possess only real alternating zeros.[64] Precisely, for an *even* density (21),

$$\begin{gathered} D_0 = 1, \quad D_1(z) = z, \quad D_2(z) = z^2-\omega_1^2, \\ D_3(z) = z\left(z^2-\omega_2^2\right), \ldots, \\ E_0 = 0, \quad E_1 = C_0, \quad E_2(z) = C_0 z, \\ E_3(z) = C_0\left(z^2-\left(\omega_2^2-\omega_1^2\right)\right), \ldots, \end{gathered} \tag{30}$$

with the characteristic frequencies [(8) and (9)] so that

$$\omega_2^2-\omega_1^2 = \frac{1}{C_0C_2^2}\left[\det\begin{pmatrix} C_0 & 0 & C_2 \\ 0 & C_2 & 0 \\ C_2 & 0 & C_4 \end{pmatrix}\right] \ge 0. \tag{31}$$

This last inequality stems from the Hölder or Cauchy–Bunyakovsky–Schwarz inequality[40,60] with the equality taking place when $q = 0$. For more details, see Refs. 65 and 70. The positivity of the difference (31) was employed in Refs. 16, 17, and 63 to control the quality of different numerical methods of calculation of OCP static structural characteristics.

Observe that the inequality (31) also implies the solvability condition of the Hamburger truncated moment problem so that by virtue of Eq. (28) for $\upsilon = 2$, using the Sochocki–Plemelj–Dirac formula

$$\frac{1}{\omega'-\omega-i0^+} = \frac{\mathscr{P}}{\omega'-\omega} + \pi i\delta(\omega'-\omega) \tag{32}$$

($\mathscr{P}$ standing for the Cauchy principal value), and the polynomials (30) we immediately obtain the loss function

$$\begin{aligned} \frac{\mathscr{L}_2(q,\omega)}{C_0(q)} &= \mathrm{Im}\frac{\omega_2^2-\omega_1^2-\omega(\omega+R_2)}{\omega\left(\omega^2-\omega_2^2\right)+R_2\left(\omega^2-\omega_1^2\right)} \\ &= \frac{\omega_1^2\left(\omega_2^2-\omega_1^2\right)\mathrm{Im}R_2}{\left|\omega\left(\omega^2-\omega_2^2\right)+R_2\left(\omega^2-\omega_1^2\right)\right|^2}, \quad \omega = Re(z+i0^+). \end{aligned} \tag{33}$$

This expression involves the Nevanlinna parameter function, which acquires now the dependence on the dimensionless wavenumber q, and which we model here by its static value

$$R_2(0,q) = ih_0(q), \quad h_0(q) > 0. \tag{34}$$

The latter was determined in Ref. 16 on the basis of a physical observation (the loss function possesses an extremum at $\omega = 0$) in terms of the characteristic frequencies $\omega_1(q)$ and $\omega_2(q)$

$$h_0(q) = \frac{\omega_2^2(q)}{\sqrt{2}\omega_1(q)}, \tag{35}$$

so that

$$\frac{\mathscr{L}_2(q,\omega)}{C_0(q)} = \frac{\omega_1^2\left(\omega_2^2-\omega_1^2\right)h_0}{\omega^2\left(\omega^2-\omega_2^2\right)^2+h_0^2\left(\omega^2-\omega_1^2\right)^2}. \tag{36}$$

Hence, due to the Kramers–Kronig relations, we obtain the following model for the inverse dielectric function:

$$\begin{aligned} \varepsilon^{-1}(q,\omega) &= 1+\frac{\omega_p^2\left(\omega+ih_0(q)\right)}{\omega\left(\omega^2-\omega_2^2(q)\right)+ih_0(q)\left(\omega^2-\omega_1^2(q)\right)} \\ &= 1+\frac{\omega_p^2\left(\sqrt{2}\omega\omega_1(q)+i\omega_2^2(q)\right)}{\sqrt{2}\omega\omega_1(q)\left(\omega^2-\omega_2^2(q)\right)+i\omega_2^2(q)\left(\omega^2-\omega_1^2(q)\right)}. \end{aligned} \tag{37}$$

Notice that, in general, this (inverse) dielectric function satisfies the sum rules for any Nevanlinna parameter function from a certain (Nevanlinna[64]) mathematical class. It is shown in Sec. 2.1 of the supplementary material how solution (36) converts into (22) if we neglect the energy dissipation, i.e., consider the limiting form of Eq. (36) when $\mathrm{Im}R_2(\omega,q) \to 0$.

In what follows, we present various methods of calculation of the system static structure factor, the frequency $\omega_1(q)$, the static dielectric function, and the screened susceptibility compared to the available numerical data.

C. Taking the energy dissipation into account

The dynamic properties of the quantum Coulomb systems we try to describe here include not only the dynamic structure factor stemming from Eqs. (5) and (33) or (36) but also the complex frequencies of the collective modes existing in the system: the unshifted (diffusion) and shifted ones,

$$\omega_{\rm us}(q) = -ia(q)\,; \quad \omega_{\pm\rm sh}(q) = \pm W(q) - ib(q). \tag{38}$$

These parameters are to be obtained by resolving the dispersion equation $\varepsilon(q,z)=0$ or

$$\sqrt{2}z\omega_1(q)\left(z^2-\omega_2^2(q)\right)+i\omega_2^2(q)\left(z^2-\omega_1^2(q)\right)=0, \tag{39}$$

exactly, using the Cardano formulas (see Refs. 16 and 71)

$$\begin{aligned}\omega_{\rm us}(q) &= -ia(q) = -w^2X - wY - ih_0/3,\\ \omega_{-\rm sh}(q) &= -W(q) - ib(q) = -X - Y - ih_0/3,\\ \omega_{\rm sh}(q) &= W(q) - ib(q) = -wX - w^2Y - ih_0/3.\end{aligned} \tag{40}$$

Here, $w=\exp(2\pi i/3)$ and

$$\begin{aligned}X=\sqrt{h_0V^2/2i+Z^3}3, \quad Y=\sqrt{h_0V^2/2i-Z^3}3,\\ Z^3=\sqrt{-\left(\omega_2^2/3-h_0^2/9\right)^3-\left(h_0V^2/2\right)^2},\\ V^2=-\omega_2^2/3+\omega_1^2+2h_0^2/27,\end{aligned} \tag{41}$$

the intrinsically positive decay parameters $a(q)$ and $b(q)$ in Eq. (38) being the decrements of the corresponding collective modes. If these decrements are relatively small, the above canonical solutions are applicable and relation (24) is valid. The energy dissipation processes can be accounted for to specify relation (24). To this end, one can integrate the $\upsilon=2$ expression for the dynamic structure factor

$$S(q,\omega)=\frac{q^2n}{3\pi\Gamma}\frac{\omega_p^2\left(\omega_2^2-\omega_1^2\right)h_0B(\beta\hbar\omega)}{\omega^2\left(\omega^2-\omega_2^2\right)^2+h_0^2\left(\omega^2-\omega_1^2\right)^2} \tag{42}$$

analytically. Thus, an equation relating the characteristic frequency $\omega_1(q)$ to $\omega_2(q)$ and the measurable SSF $S(q)$ can be obtained, see Sec. 1 in the supplementary material. This allows for the incorporation of additional information not related to the sum rules or the moments and taking the energy dissipation into account. In Sec. V, we provide a numerical solution for the characteristic frequency $\omega_1(q)$ compared to the similar results obtained by other methods described there.

We observe that the above relations between the characteristic frequencies $\omega_1(q)$ and $\omega_2(q)$ and the SSF close our algorithm of calculation of the static properties, which permits one to express the latter in terms of the SSF data determined independently. The interconnections between the frequencies $\omega_1(q)$ and $\omega_2(q)$ are effectively relations between the moments (or sum rules) $C_0(q)$ and $C_4(q)$ since the moment $C_2=\omega_p^2$ is the f-sum rule, which is the density conservation law. The frequency $\omega_1(q)$ is directly related to the system static dielectric function, see Eqs. (8) and (11), while $\omega_2(q)$ is determined by the static structure factor [the moment (10)], via Eqs. (9), (13), and (15). Thus, the established relations between the frequencies $\omega_1(q)$ and $\omega_2(q)$ provide connections between the static dielectric function and the static structure factor, and they are extensions of the classical relation, which follows from Eq. (25)

$$\varepsilon^{-1}_{\rm classical}(q,0)=1-\frac{3\Gamma S(q)}{q^2}.$$

The first of these extensions is Eq. (26); we can observe that

$$\frac{\beta\hbar\omega_p^2}{2\omega_2}\coth\frac{\beta\hbar\omega_2}{2}-\frac{\omega_p^2}{\omega_2^2}\underset{\hbar\to0}{\simeq}\frac{\left(\beta\omega_p\hbar\right)^2}{12}+O(\hbar^4).$$

The energy dissipation processes are not included in the derivation of Eq. (26). The second one is obtained implicitly by the frequency integration of Eq. (42); it is demonstrated in the supplementary material [Eq. (12)] that if the static NPF imaginary part $h_0(q)$ responsible in our model for the energy dissipation decreases, the second relation between the static dielectric function and the static structure factor of a quantum liquid of charged fermions reduces to Eq. (26). In addition, we show in Sec. V that even if we use instead of a proper SSF some fitting (see Sec. IV) formally valid in classical one-component plasmas only, the results for the static characteristics are still in agreement with the PIMC data.

IV. ADDITIONAL THEORETICAL ALGORITHMS

A. The local-field corrected RPA

Here, we want to update the extended-RPA approach to the calculation of the quantum Fermi liquid SSF and the radial distribution function (RDF), particularly, the zero-separation value of the latter, $g(0)$, introduced in Ref. 72 and applied in Ref. 73. The dynamic local-field correction (DLFC) function and its relation to the Nevanlinna parameter function are discussed in Ref. 18. Contemporary simulation data on the DLFC can be found in Ref. 20. Here, like in Ref. 9, we employ the static local-field correction function approximation. Then, the electron liquid static structure factor is defined as in Ref. 10,

$$S(q)=\frac{1}{\beta n}\sum_{l=-\infty}^{\infty}\frac{\Pi_0(q,z_l)}{1+\phi(q)\left(1-G(q)\right)\Pi_0(q,z_l)}, \tag{43}$$

where $\phi(q)=4\pi e^2a^2/q^2$, $G(q)$ is the static local-field correction function and $\Pi_0(q,z_l)$ is the polarization function in the random-phase approximation[39,40] at the Matsubara frequencies $z_l=2\pi il/\beta\hbar$. As to $G(q)$, here we use the model suggested back in Ref. 72,

$$G(q)=\frac{q^2}{\mathfrak{a}q_s^2+\mathfrak{b}q^2}, \tag{44}$$

where

$$\mathfrak{b}=\left[1-g(0)\right]^{-1}, \tag{45}$$

$$g(0)=1+\frac{2}{3\pi}\int_0^\infty\left(S(p)-1\right)p^2dp, \tag{46}$$

which is the zero-distance value of the radial distribution function

$$q_s^2=\sqrt[3]{\frac{18}{\pi^2}}\sqrt{\theta}\mathrm{F}_{-1/2}(\eta)\mathrm{r_s},$$

and the parameter $\mathfrak{a}$ is determined from the compressibility sum rule

$$\lim_{q\to 0}\left(\frac{q^2}{q_D^2}\right)^{-1}\left(\frac{q^2}{\mathfrak{a}q_s^2+\mathfrak{b}q^2}\right)=1-\beta\left(\frac{\partial P}{\partial n}\right)_\beta.$$

Notice that

$$\frac{q_D^2}{q_s^2}=\frac{4}{3}\theta^{-\frac{3}{2}}F_{-1/2}^{-1}(\eta),$$

where $q_D^2=3\Gamma$ is the Debye dimensionless wavenumber squared, and that in the present work, we make use of the equation of state of the paramagnetic UEG

$$P=\frac{n}{\beta}+\frac{n}{3\beta}\left(2f(r_s,\theta)+r_s\frac{\partial f(r_s,\theta)}{\partial r_s}\right),$$

found in Ref. 19 by the PIMC simulation method. In addition, to avoid inconsistencies related to $g(0)$, we carried out the reiteration procedure via Eqs. (43)–(46). This procedure turned out to be rapidly convergent, and the results for the parameter $g(0)$ are presented in Sec. V C in comparison with alternative relevant data. Comparison of these results to the recent PIMC data on $g(0)$[23] is beyond the scope of the present work.

B. Static structure factor fitting models

In our calculations, we were also employing two different fittings of the modified hypernetted-chain (MHNC) results. The first fitting was obtained by Bretonnet and Derouiche.[74] The authors of that work used the direct correlation function $c(r/a)$ in a form consistent with features of the one-component plasma and derived a simple analytic expression for the OCP SSF $S(q)$

$$S(q)=\left(1-\frac{3\Gamma}{q^4\alpha_2^2}\left[\cos(q\alpha_1)+2\cos(q\alpha_2)-3\frac{\sin(q\alpha_1)}{q\alpha_1}\right]\right)^{-1}. \quad (47)$$

This relation (47), which satisfies the perfect screening condition,

$$S(q\to 0)\simeq\frac{q^2}{3\Gamma},$$

was then fitted to the modified hyper-netted-chain data of the classical one-component plasma SSF, tabulated by Rogers *et al.*[75] for $0.1\le q\le 25.0$ and $0.1\le\Gamma\le 180$. Some 8 years later, Young *et al.*[76] used a nonlinear least squares fitting program to find an analytic fit to the classical one-component plasma SSF $S(q)$ over the ranges $0\le q\le 21.75$ and $1\le\Gamma\le 225$. The $S(q)$ function was generated in that work as a table stemming from the solution of the modified hypernetted chain integral equation, and the table was fitted with polynomials in q and Γ, using a total of 175 coefficients. Though these fittings were designed for classical OCPs, overall agreement with alternative results is quite satisfactory.

V. NUMERICAL RESULTS

We have constructed two different approaches to the determination of the characteristic frequency

$$\omega_1(q)=\frac{\omega_p}{\sqrt{1-\varepsilon^{-1}(q)}}$$

and, hence, of the static dielectric function $\varepsilon(q)$ and the static screened response function

$$\chi(q)=\frac{q^2}{3\Gamma}\left(1-\varepsilon^{-1}(q)\right). \quad (48)$$

The first approach is obtained from a specific, physically motivated *canonical* solution (22) of the Hamburger truncated moment problem, and it does not take the energy dissipation in the system into account. The second one is based on the *non-canonical* solution of this moment problem and does account for the energy dissipation processes in the system, and this approach is described in Sec. III C. Its idea is to integrate Nevanlinna's five-moment expression for the dynamic structure factor specified by the static model for the Nevanlinna parameter function [(34) and (35)] analytically and to equalize the integral which depends only on the frequencies $\omega_1(q)$ and $\omega_2(q)$ to a model SSF. The latter can be precalculated using the same SSF, Eqs. (9) and (13)–(15). Thus, an equation is obtained with a unique unknown variable, the frequency $\omega_1(q)$, and this procedure is described in detail in Sec. III C. We have solved this equation numerically by the program Mathematica and have determined other static characteristics. Then we have compared these results to the PIMC data for a uniform warm dense electron gas. To this end, we had to employ some models of the Fermi liquid static structure factor $S(q)$. In these calculations, $S(q)$ was evaluated by four different algorithms discussed above: (i) using the SSF found by the PIMC method itself, the corresponding results are labeled in Figs. 1–8 "Groth model," see Ref. 19; (ii) with the proper SSF evaluated in the extended temperature-dependent random-phase approximation[72] using the data on the correlation free energy of Ref. 6 by the procedure described in Sec. IV A, in these cases the label "Adamjan model" was used. The labels "Bretonnet model" and "Young model" correspond to the same procedure but using (iii) the SSF data of Ref. 74 and (iv) the SSF data of Ref. 76, respectively. In addition, we have also used the standard random-phase SSF so that in what follows in each figure, there appear six types of symbols, since all these theoretical results are compared in Figs. 1–8 to the data we had calculated for each static characteristic from the corresponding "PIMC 2020" in Ref. 7.

Thus, we present in what follows six different sets of data. To avoid confusion, we have separated the "canonical" and "non-canonical" sets.

A. Without energy dissipation

This approach is based on relation (24)

$$\omega_1(q)=\frac{\omega_2(q)}{\sqrt{1+\frac{3\Gamma\omega_2^2(q)}{q^2\omega_p^2}S(q)-\frac{\beta\hbar\omega_2(q)}{2}\coth\frac{\beta\hbar\omega_2(q)}{2}}}. \quad (49)$$

We observe in Figs. 1–4 that up to $q=6$ and at higher values of the coupling parameter Γ, there are no discrepancies in the values of the frequency $\omega_1(q)$ obtained using the static structure factor of different models; at higher wavenumbers, only the RPA SSF leads to the values of this frequency very close to the PIMC data. All these differences do not manifest themselves in the results for the dielectric function, but the response function proves to be sensitive to the SSF employed

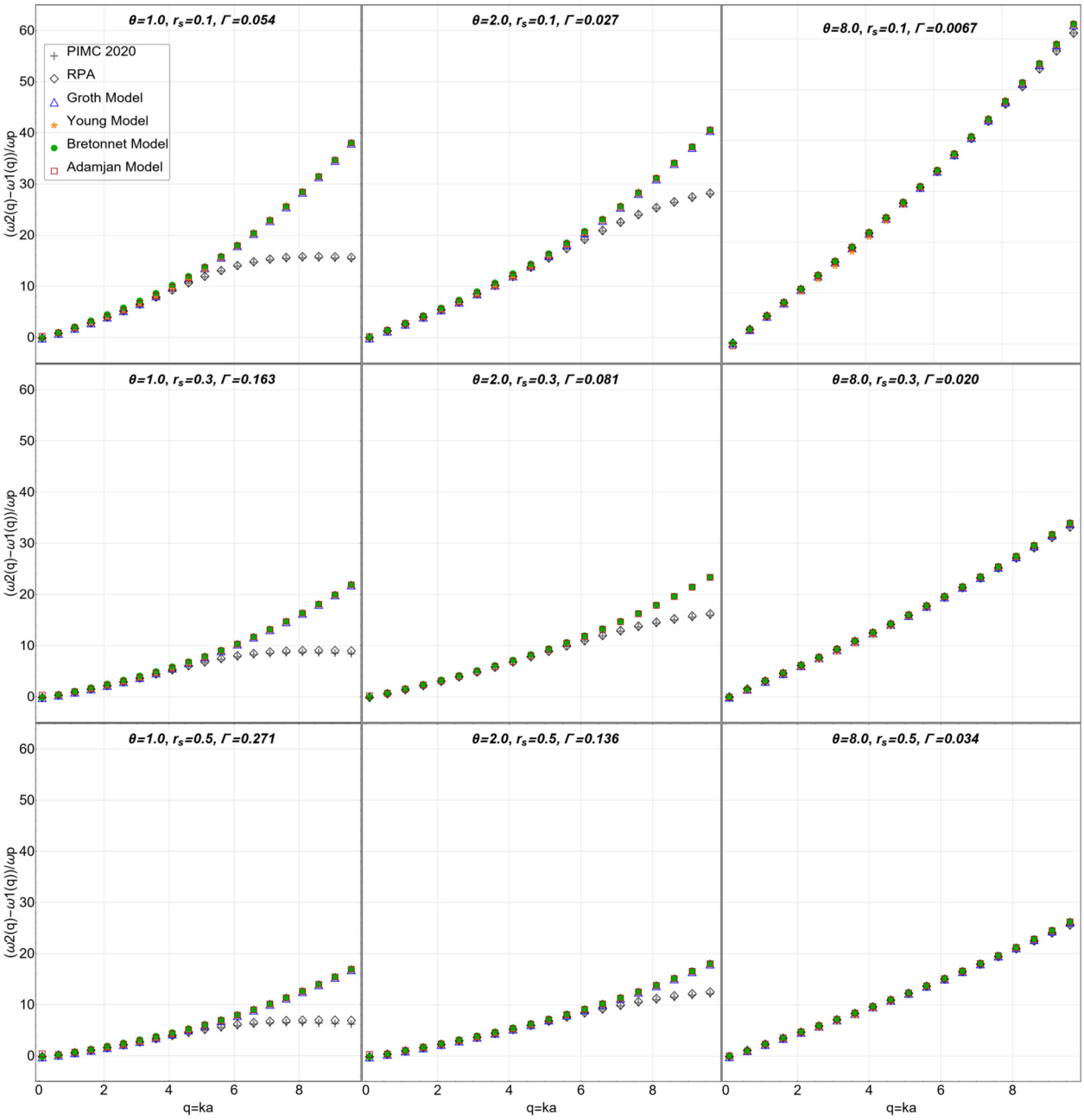

FIG. 1. The values of the difference $\omega_2(q) - \omega_1(q)$ at different values of r_s and θ. Here and in the rest of the figures, the data marked "Groth model," "Bretonnet model," and "Young model" correspond to the results of Refs. 19, 74, and 76, respectively, as it is explained in the text; the results labeled "Adamjan model" were obtained within the extended random-phase approximation,[72] "PIMC 2020" were obtained from Ref. 7, and results marked "RPA" correspond to the SSF in the standard random-phase approximation. All calculations were carried out within the "canonical" approximation using relation (49) without taking into account the energy dissipation in the system.

at higher Γ, except for the RPA prediction. The inequality $\omega_2(q) - \omega_1(q) \geq 0$ (31), which is equivalent to the Hölder or Cauchy–Bunyakovsky–Schwarz inequalities in L^2, and is also the condition of solvability of the five-moment Hamburger moment problem (18), see Fig. 1, is satisfied in all cases we have considered. We notice that the energy dissipation neglected in all non-RPA models affects the results quite significantly at higher coupling and wavenumbers. It is curious that intrinsically classical fitting models from Refs. 74 and 76 seem to produce relatively reliable results for the UEG static characteristics.

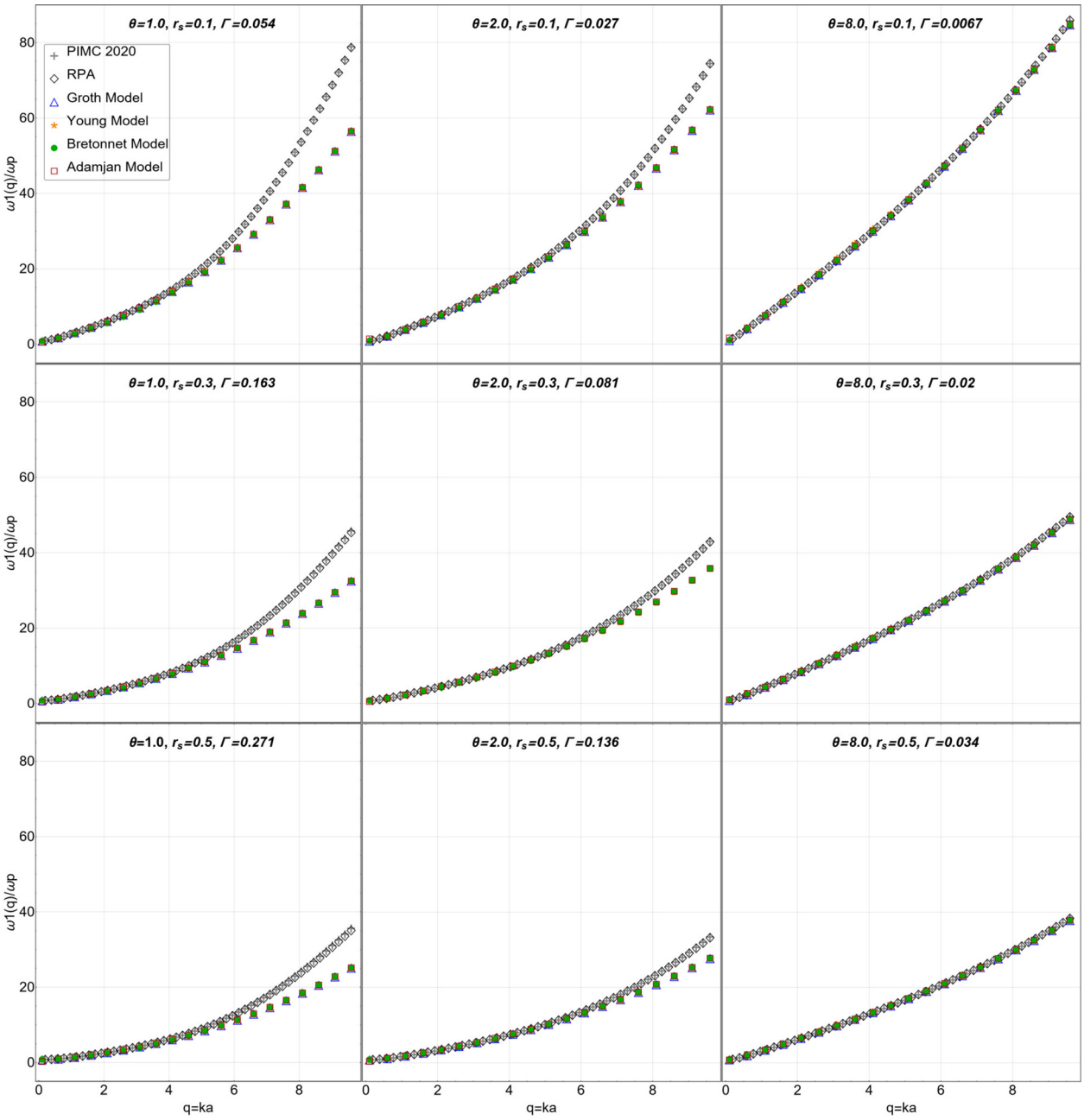

FIG. 2. The values of the frequency $\omega_1(q)$ at different values of r_s and θ. Notations are as in Fig. 1. In all calculations, dissipationless relation (49) was used.

B. With energy dissipation

This approach presented in Sec. III C is described in detail in the supplementary material, Sec. I. The results obtained within this method of evaluation of static characteristics of quantum liquids of charged fermions, at least in the case of a warm dense UEG, prove to be in quantitative agreement with the PIMC and RPA data, and slight deviations in the values of the response function are within the calculation precision. It is interesting that the results of theoretical calculation of $\varepsilon(q)$ effectively coincide even if we employ the classical SSF fittings, like in the dissipationless "canonical" case. This implies that we are in a position to predict the static dielectric function of a warm dense

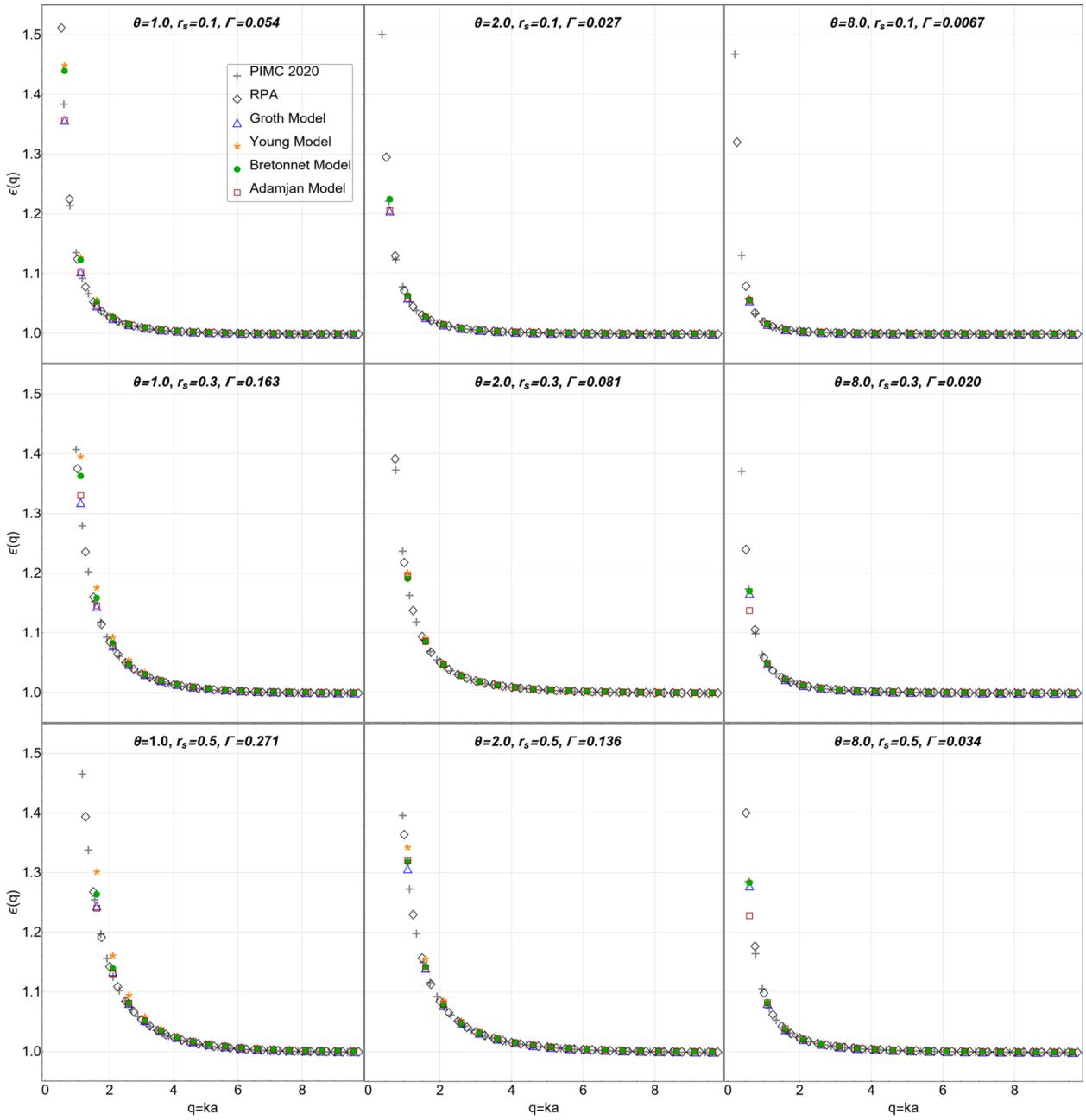

FIG. 3. The values of the static dielectric function $\varepsilon(q) = \varepsilon(q, 0)$ at different values of r_s and θ. Notations are as in Fig. 1. In all calculations, dissipationless relation (49) was used.

quantum uniform electron gas without carrying out the PIMC simulations. Once more we observe that in all cases considered inequality (31) holds.

The numerical PIMC simulations have been carried out with a limited number of particles (N = 54 particles in Ref. 23), and due to the fermion sign problem, these simulations were restricted to small coupling parameters, $r_s \lesssim 0.7$. To extend the range of parameters, the authors of the simulations have to perform simulations with an even smaller number of particles. They claim[6,77] that the data on the static structure factor only weakly depend on the particle number, but we believe that the N-dependence and the limited range of variation of the coupling parameter r_s are intrinsic difficulties of the *ab initio* PIMC simulation method. Thus, the possibility to complement the PIMC simulations with the method-of-moments data, especially, for

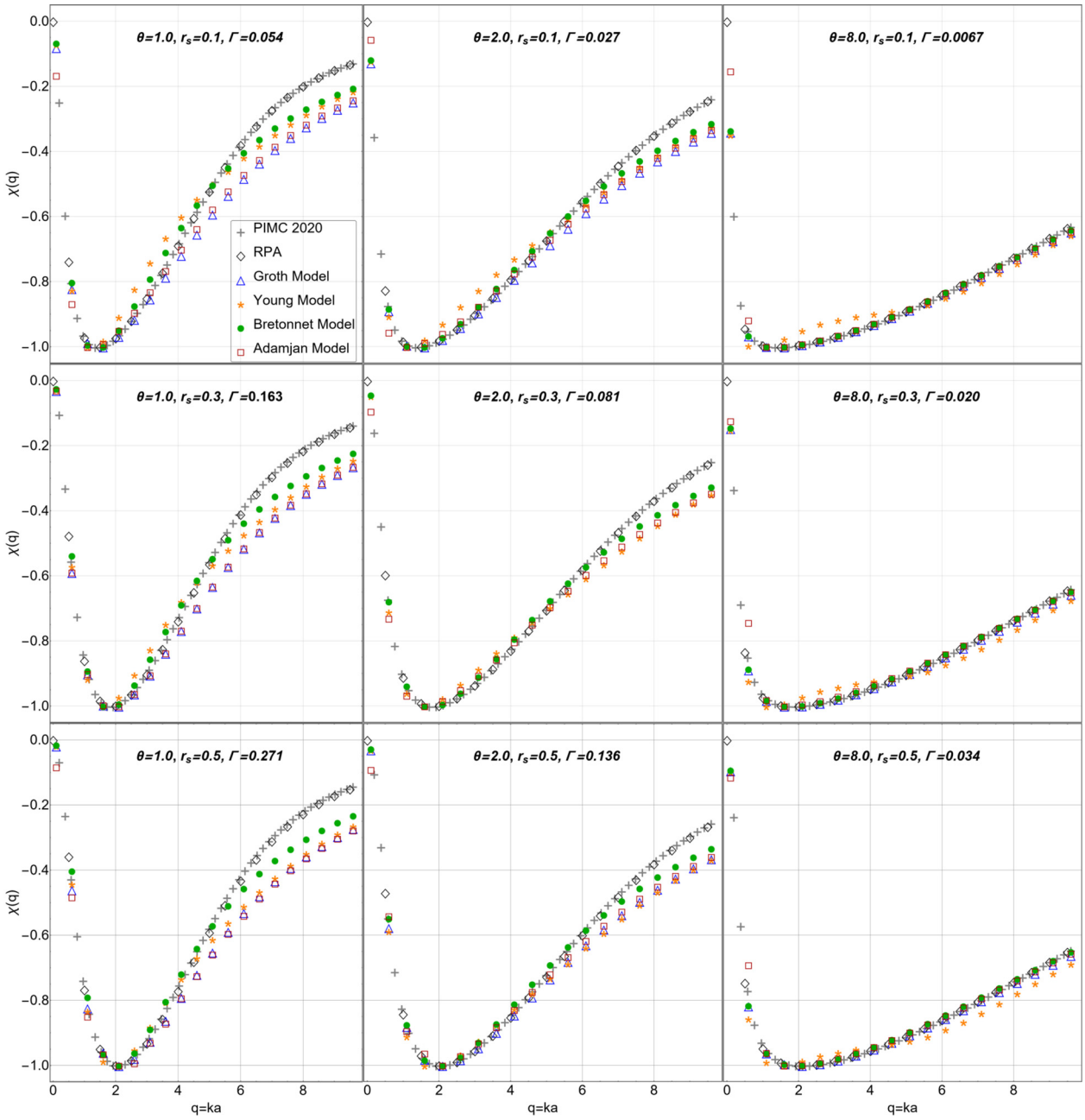

FIG. 4. The values of the screened susceptibility (48) at different values of r_s and θ. Notations are as in Fig. 1. In all calculations, dissipationless relation (49) was used.

moderately and strongly coupled Fermi liquids, acquires an additional importance.

Finally, and these are the main results of the present work, we compared the calculated values of the frequency $\omega_1(q)$ (Fig. 2), the static values of the dielectric function $\varepsilon(q) = \varepsilon(q;0)$ (Fig. 3), and of the screened response function (Fig. 4) widely used in Refs. 1 and 7 to those obtained in these papers within the *ab initio* path-integral quantum Monte Carlo approach and in the temperature-dependent random-phase approximation.

The symbols used in these figures to distinguish the data (Fig. 4) are those of Figs. 1 and 5, respectively. We observe that there is almost no discrepancy between the PIMC data and the results obtained within all theoretical models with energy dissipation.

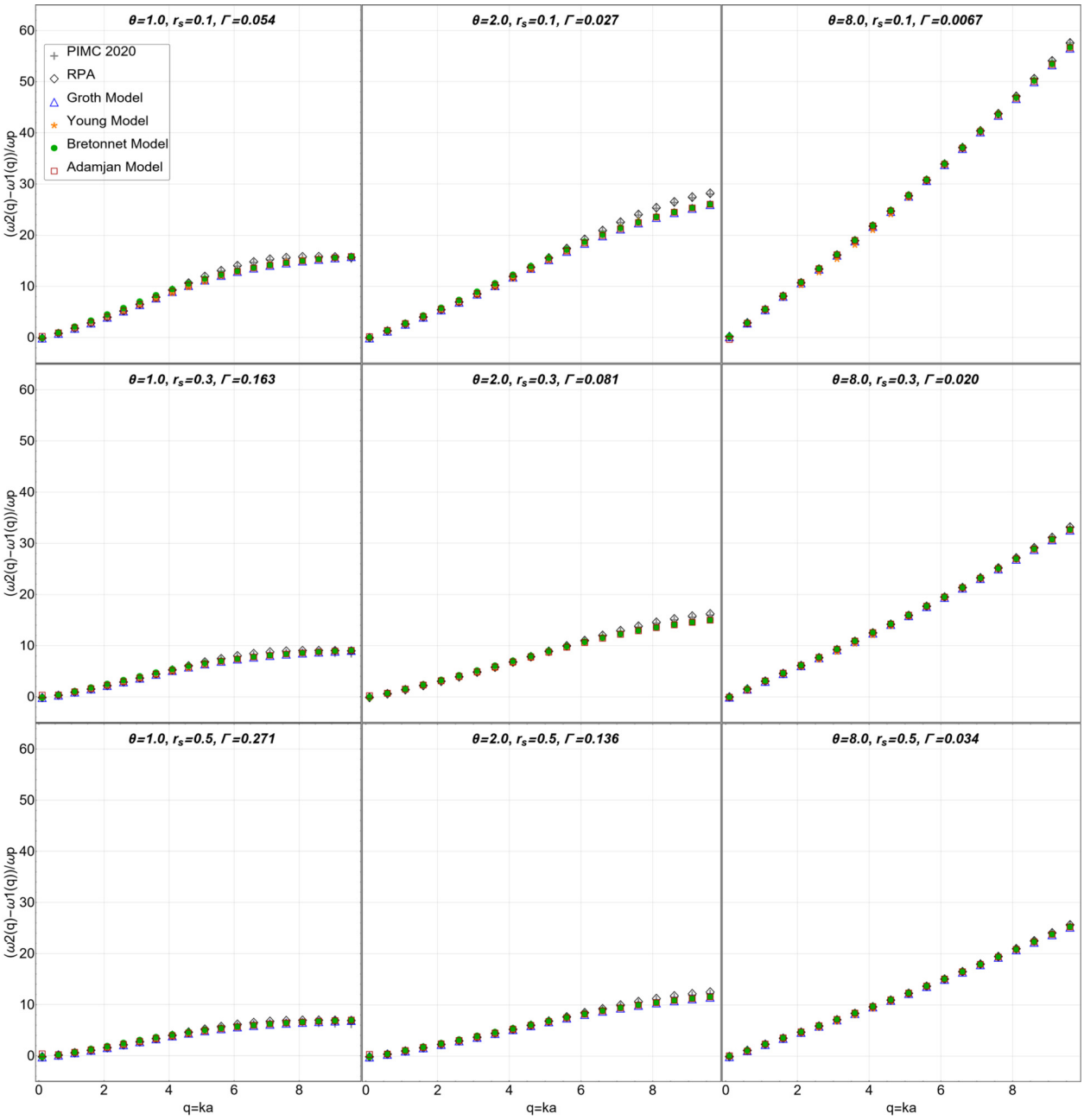

FIG. 5. The values of the difference $\omega_2(q) - \omega_1(q)$ at different values of r_s and θ. Notations are as in Fig. 1. The energy dissipation was taken into account in all calculations.

C. On the radial distribution function zero separation value

The algorithm outlined in Sec. IV A permits us to evaluate the zero-distance value of the radial distribution function $g(0)$, whose values are compared in Table I to those of the well-known expression by Yasuhara[78] (see also Refs. 34, 72, and 73) obtained by resummation of electron–electron ladder diagrams

$$g_{\mathrm{Y}}(0) = \frac{1}{8}\left[\frac{y}{I_1(y)}\right]^2, \quad y = 4\sqrt{\frac{r_s}{\pi}\sqrt{\frac{4}{9\pi}3}}, \tag{50}$$

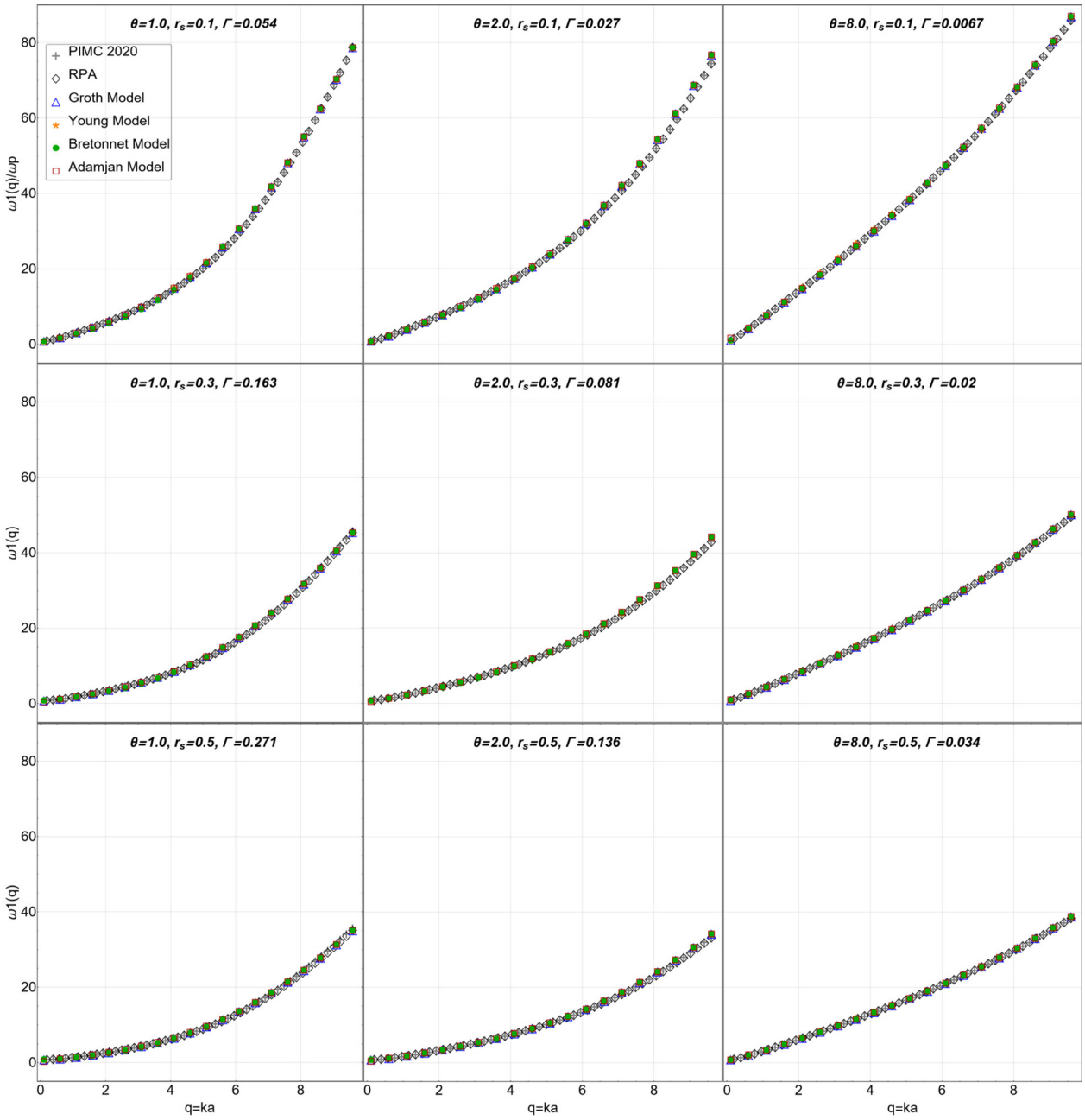

FIG. 6. The values of the frequency $\omega_1(q)$ at different values of r_s and θ. Notations are as in Fig. 1. In all calculations, the energy-dissipation processes in the system were accounted for.

where

$$I_1(y) = \frac{1}{\pi}\int_0^{\pi} \exp(y\alpha)\cos\alpha d\alpha$$

is the first-order first-kind modified Bessel function.

From Table I, we observe that under the above conditions, the values obtained within the extended approach of Sec. IV A are very close to the PIMC data of Ref. 19, and both are quite close to the ground state prediction of Eq. (50), label $g_Y(0)$. The classical fittings of Refs. 74 and 76, which depend only on Γ, lead to the "classical" values that are closer to 1.0, though a more precise fitting of Ref. 76 does it to a lesser extent. Nevertheless, the results presented in Table I are collateral, and they are to be compared to the new results of Ref. 23 in a separate paper.

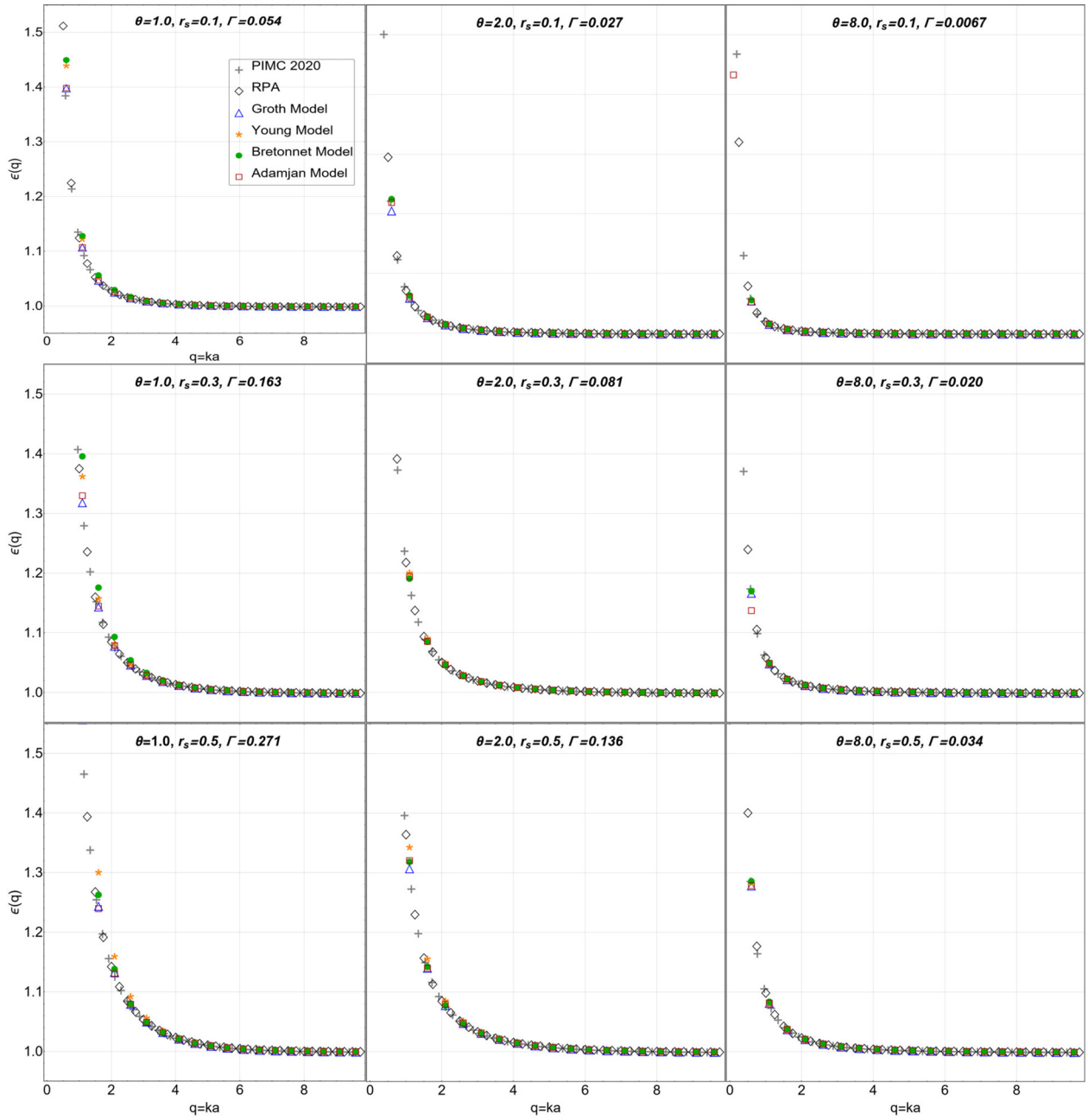

FIG. 7. The values of the static dielectric function $\varepsilon(q) = \varepsilon(q, 0)$ at different values of r_s and θ. Notations are as in Fig. 1. In all calculations, the energy-dissipation processes in the system were accounted for.

VI. CONCLUSIONS

Two versions of direct relations between the minus first and third frequency power moments of the dynamic structure factor of a quantal normal liquid of charged fermions or sum rules are found. These relations effectively connect the system static dielectric funtion and the zeroth moment or the static structure factor. These connections in the case of a warm dense electron gas are checked against the recent numerical data obtained within the path-integral Monte Carlo method. The quantitative agreement achieved in the present work implies the possibility to evaluate the static characteristics of an electron gas under the conditions inaccessible for the simulations as soon as the corresponding static structure factor is available. Numerical agreement is attained even if the employed static structure factor is

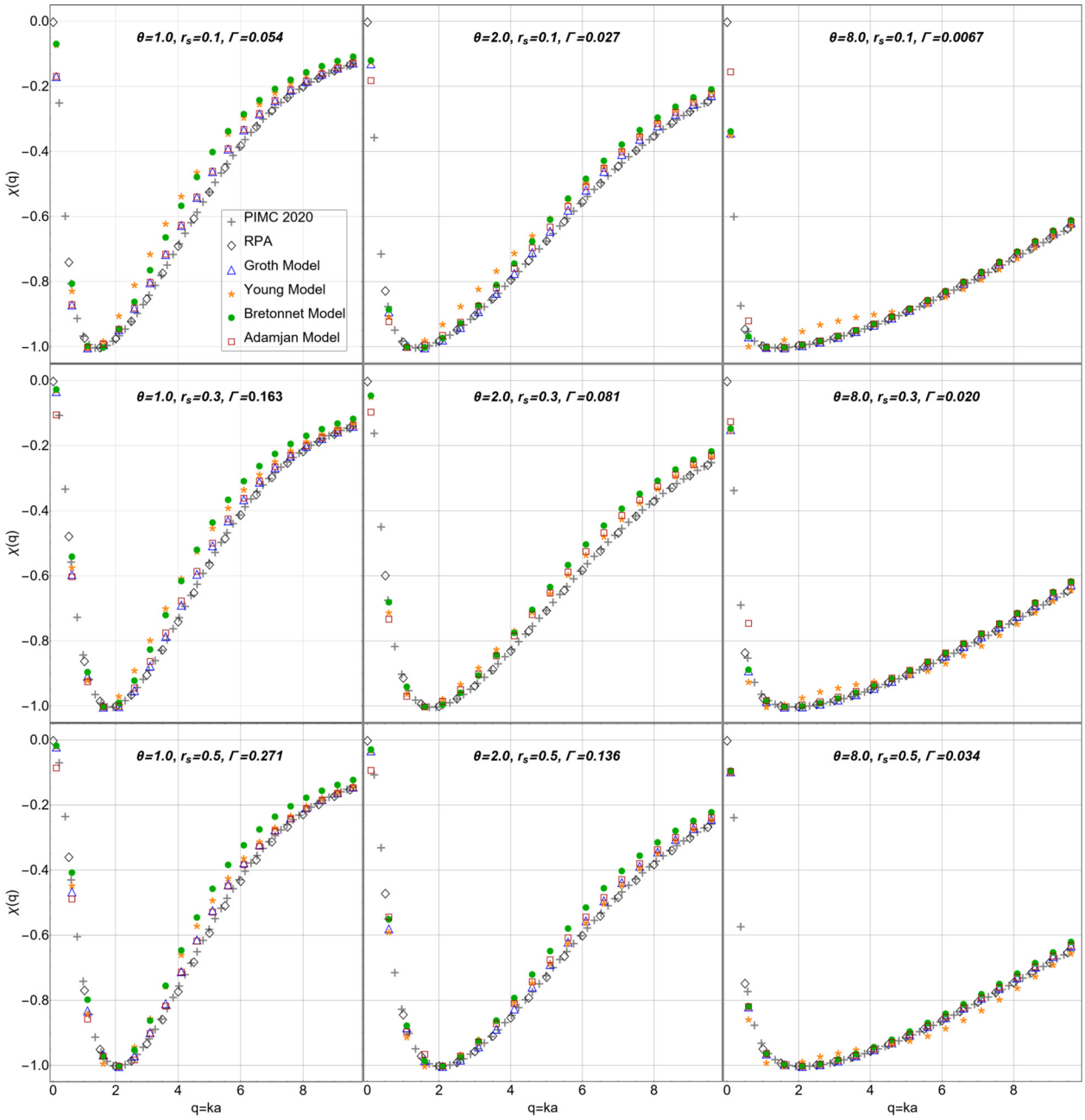

FIG. 8. The values of the screened susceptibility (48) at different values of r_s and θ. Notations are as in Fig. 1. In all calculations, the energy-dissipation processes in the system were accounted for.

obtained by a version of the intrinsically classical hyper-netted-chain approach. This also confirms the applicability and robustness of the employed version of the moment method. An alternative self-consistent model,[72] see Sec. IV A, using a specific form for the static local-field correction involving the path-integral Monte Carlo data for the uniform electron gas compressibility and the traditional Matsubara-frequency summation, proved to be insufficient to describe the gas static characteristics. A close agreement with the RPA results is not astonishing since the warm-dense matter conditions are within the realm of applicability of the random-phase approximation. Perhaps, the local-field corrections suggested in Refs. 20–22 (see also references therein) could provide a similar level of quantitative agreement, but this is a topic of a subsequent publication. The model we employed for the dynamic structure factor can be further compared to the PIMC

TABLE I. Some results on the radial distribution function zero-distance value, $g(0)$.

Γ	θ	r_s	$g(0)$ (Ref. 73)	$g(0)$ (Ref. 19)	$g(0)$ (Ref. 75)	$g(0)$ (Ref. 77)	$g_{\mathrm{Y}}(0)$
0.054	1	0.1	0.459	0.461	0.954	0.685	0.468
0.027	2	0.1	0.467	0.468	0.971	0.728	0.468
0.013	4	0.1	0.476	0.477	0.987	0.736	0.468
0.007	8	0.1	0.497	0.498	0.993	0.736	0.468
0.163	1	0.3	0.383	0.398	0.889	0.471	0.411
0.047	4	0.3	0.427	0.429	0.964	0.709	0.411
0.020	8	0.3	0.449	0.451	0.981	0.733	0.411
0.271	1	0.5	0.297	0.347	0.837	0.345	0.362
0.136	2	0.5	0.344	0.361	0.903	0.515	0.362
0.068	4	0.5	0.383	0.388	0.945	0.656	0.362
0.034	8	0.5	0.416	0.417	0.969	0.719	0.362

data on the UEG dynamic properties;[20,21] it also determines the static screening effects in the electron gas. On the other hand, further development of the present results might consist in incorporating higher-order power moments related to the multipoint static structure factors $S(\mathbf{k}_1, \mathbf{k}_2)$, $S(\mathbf{k}_1, \mathbf{k}_2, \mathbf{k}_3)$, etc., scarcely known at the moment. This task is also beyond the scope of the present work.

Finally, our approach is valid for zero-temperature, magnetized, and/or multi-component Coulomb systems as well. In the latter two cases, the matrix version of the method of moments developed earlier[79] can be applied. An extension of the present method to the determination of the dynamic structure factor and other dynamic characteristics of Fermi liquids of charged particles has been recently reported at the International Conference on the Physics of Non-Ideal Plasmas (PNP 17) in Dresden, Germany. Corresponding detailed publications including comparison with alternative approaches based on Green's functions[80–83] or the local-field corrected random-phase approximation[84] are due.

SUPPLEMENTARY MATERIAL

See the supplementary material for some mathematical details of procedures described in the main text. It also includes some results from Refs. 24 and 25.

ACKNOWLEDGMENTS

I.M.T. is grateful to M. Bonitz and T. Dornheim for several valuable discussions. The authors appreciate that M. Bonitz and T. Dornheim provided accurate path integral Monte Carlo simulation results. I.M.T. also acknowledges fruitful discussions with Yu. V. Arkhipov and L. Conde and the financial support provided by the Committee of Science of the Ministry of Education and Science of the Republic of Kazakhstan (Project No. AP09260349).

AUTHOR DECLARATIONS

Conflict of Interest

The authors have no conflicts to disclose.

DATA AVAILABILITY

The data that support the findings of this study are available from the corresponding author upon reasonable request.

REFERENCES

[1]T. Dornheim, S. Groth, and M. Bonitz, Phys. Rep. **744**, 1 (2018).
[2]L. H. Thomas, Proc. Cambridge Phil. Soc. **23**, 542 (1927); E. Fermi, Z. Phys. **48**, 73 (1928).
[3]P. Hohenberg and W. Kohn, Phys. Rev. **136**, 3864 (1964).
[4]W. Kohn and L. J. Sham, Phys. Rev. **140**, A1133 (1965).
[5]V. L. Lignères and E. A. Carter, "*An Introduction to Orbital Free Density Functional Theory*," in *Handbook of Materials Modeling*, edited by S. Yip (Springer, Netherlands), pp. 137–148.
[6]T. Dornheim, S. Groth, T. Sjostrom, F. D. Malone, W. M. C. Foulkes, and M. Bonitz, Phys. Rev. Lett. **117**, 156403 (2016).
[7]T. Dornheim, Zh. A. Moldabekov, and J. Vorberger, arXiv:2003.00858v1 (2020).
[8]L. Shen and W. Yang, J. Chem. Theory Comput. **14**(3), 1442 (2018).
[9]K. S. Singwi, M. P. Tosi, R. H. Land, and A. Sjölander, Phys. Rev. **176**, 589 (1968).
[10]S. Tanaka and S. Ichimaru, J. Phys. Soc. Jpn. **55**, 2278 (1986).
[11]Ph. Nozières and D. Pines, *Theory of Quantum Liquids* (Avalon Publishing, 1999).
[12]G. Kalman and K. I. Golden, Phys. Rev. A **41**, 5516 (1990); K. I. Golden and G. J. Kalman, Phys. Plasmas **7**, 14 (2000); *ibid.* **8**, 5064 (2000).
[13]L. P. Kadanoff and P. C. Martin, Ann. Phys. (N. Y.) **24**, 419 (1963).
[14]P. C. Martin and S. Yip, Phys. Rev. **170**, 151 (1968).
[15]V. D. Gorobchenko and E. G. Maksimov, Usp. Fiz. Nauk **130**, 65 (1980), [in English: Sov. Phys. Usp. **23**, 35 (1980)].
[16]Yu. V. Arkhipov, A. Askaruly, A. E. Davletov, D. Yu. Dubovtsev, Z. Donkó, P. Hartmann, I. Korolov, L. Conde, and I. M. Tkachenko, Phys. Rev. Lett. **119**, 045001 (2017).
[17]Yu. V. Arkhipov, A. Askaruly, A. E. Davletov, D. Yu. Dubovtsev, Z. Donkó, P. Hartmann, I. Korolov, L. Conde, and I. M. Tkachenko, Phys. Rev. Lett. **119**, 045001 (2017).
[18]Yu. V. Arkhipov, A. Ashikbayeva, A. Askaruly, A. E. Davletov, D. Yu. Dubovtsev, Kh. S. Santybayev, S. A. Syzganbayeva, L. Conde, and I. M. Tkachenko, Phys. Rev. E. **102**, 053215 (2020).
[19]T. Dornheim, S. Groth, T. Schoof, C. Hann, and M. Bonitz, Phys. Rev. B **93**, 205134 (2016).
[20]P. Hamann, T. Dornheim, J. Vorberger, Zh. A. Moldabekov, and M. Bonitz, Phys. Rev. B **102**, 125150 (2020).
[21]P. Hamann, J. Vorberger, T. Dornheim, Zh. A. Moldabekov, and M. Bonitz, Contrib. Plasma Phys. **60**, e202000147 (2020).
[22]T. Dornheim, A. Cangi, K. Ramakrishna, M. Böhme, S. Tanaka, and J. Vorberger, Phys. Rev. Lett. **125**, 235001 (2020).
[23]K. Hunger, T. Schoof, T. Dornheim, M. Bonitz, and A. Filinov, Phys. Rev. E **103**, 053204 (2001).
[24]M. Abramowitz and I. A. Stegun, *Handbook of Mathematical Functions* (Dover Publications, New York, 1970).

[25]A. P. Prudnikov, Y. A. Brychkov, and O. I. Marichev, *Integrals and Series. Elementary Functions* (Gordon and Breach, New York, 1986), Vol. 1.
[26]I. M. Tkachenko, Phys. Rev. E **57**, 3676 (1998).
[27]O. V. Dolgov, D. A. Kirzhnits, and E. G. Maksimov, Rev. Mod. Phys. **53**, 81 (1981); E. G. Maksimov and O. V. Dolgov, Usp. Fiz. Nauk **177**, 983 (2007) [in English: Phys.-Usp. **50**, 933 (2007)]
[28]V. D. Gorobchenko, V. N. Kohn, and E. G. Maksimov, "The dielectric function of the homogeneous electron gas," in *The Dielectric Function of Condensed Systems*, edited by L. V. Keldysh, D. A. Kirzhnits, and A. A. Maradudin (Elsevier Publishing, New York, 1989), Chapter 3.
[29]G. Giuliani and G. Vignale, *Quantum Theory of the Electron Liquid* (Cambridge University Press, Cambridge, 2008).
[30]J. Lindhard and K. Dan, Vidensk. Selsk. Mat. Fys. Medd. **28**(8), 1 (1954).
[31]Yu. Zaporozhets, V. Mintsev, V. Fortov, H. Reinholz, G. Rö pke, S. Rosmej, and Y. A. Omarbakiyeva, Phys. Rev. E **99**, 043202 (2019) and references therein.
[32]Yu. Zaporozhets, V. Mintsev, V. Fortov, H. Reinholz, and G. Röpke, J. Phys. Conf. Ser. **1556**, 012069 (2020).
[33]S. Ichimaru, *Statistical Plasma Physics* (Addison-Wesley, New York, 1991), Vol. 1; S. Ichimaru, *Statistical Plasma Physics: Condensed Plasmas* (Addison-Wesley, New York, 1994), Vol. II.
[34]N. D. Mermin, Phys. Rev. B **1**, 2362 (1970).
[35]A. K. Das, J. Phys. F **5**, 2035 (1975).
[36]V. Cataudella, V. Marigliano Ramaglia, and G. P. Zucchelli, Phys. Lett. A **92**, 359 (1982).
[37]F. C. Khanna and H. R. Glyde, Can. J. Phys. **54**, 648 (1976).
[38]C. Gouedard and C. Deutsch, J. Math. Phys. **19**(1), 32 (1978).
[39]N. R. Arista and W. Brandt, Phys. Rev. A **29**, 1471 (1984).
[40]Yu. V. Arkhipov, A. B. Ashikbayeva, A. Askaruly, A. E. Davletov, and I. M. Tkachenko, Phys. Rev. E **90**, 053102 (2014), *ibid.* **91**, 019903 (2015).
[41]J. Hubbard, Proc. Roy. Soc. London, Ser. A **240**, 340 (1957).
[42]D. F. DuBois, Ann. Phys. **7**, 174 (1959).
[43]M. Gell-Mann and K. A. Brueckner, Phys. Rev. **106**, 364 (1957).
[44]L. M. Falicov and V. Heine, Adv. Phys. **37**, 57 (1960).
[45]T. M. Rice, Ann. Phys. **31**, 100 (1965).
[46]D. J. W. Geldart and S. H. Vosco, Can. J. Phys. **44**, 2137 (1966).
[47]D. J. W. Geldart and R. Taylor, Can. J. Phys. **48**, 155 (1970); *ibid.* **48**, 167 (1970).
[48]A. A. Kugler, Phys. Rev. A **1**, 1688 (1970).
[49]R. W. Shaw, Jr., J. Phys. C **3**, 1140 (1970).
[50]J. C. Kimball, Phys. Rev. A **7**, 1648 (1973).
[51]J. C. Kimball, J. Phys. A **8**, 1513 (1975).
[52]A. Kugler, J. Stat. Phys. **12**, 35 (1975).
[53]N. Iwamoto, Phys. Rev. A **30**, 3289 (1984).
[54]H. K. Schweng and H. M. Böhm, Phys. Rev. B **48**, 2037 (1993).
[55]A. Kugler, J. Stat. Phys. **8**, 107 (1973).
[56]K. N. Pathak and P. Vashishta, Phys. Rev. B **7**, 3649 (1973).
[57]R. D. Puff, Phys. Rev. **137**, A406 (1965); N. Mihara and R. D. Puff, Phys. Rev. **174**, 221 (1968).
[58]N. Iwamoto, Phys. Rev. A **33**, 1940 (1986).
[59]N. Iwamoto, E. Krotscheck, and D. Pines, Phys. Rev. B **29**, 3936 (1984).
[60]V. M. Adamyan, T. Meyer, and I. M. Tkachenko, Fiz. Plazmy **11**, 826 (1985) [in English: Sov. J. Plasma Phys. **11**, 481 (1985)].
[61]T. Meyer and I. M. Tkachenko, Contrib. Plasma Phys. **25**, 437 (1985).
[62]I. Z. Fisher, *Statistical Theory of Liquids* (University of Chicago Press, 1964).
[63]Y. V. Arkhipov, A. B. Ashikbayeva, A. Askaruly, M. Bonitz, L. Conde, A. E. Davletov, T. Dornheim, D. Y. Dubovtsev, S. Groth, K. Santybayev, S. A. Syzganbayeva, and I. M. Tkachenko, Contrib. Plasma Phys. **58**, 967 (2018).
[64]M. G. Krein and A. A. Nudel'man, *The Markov Moment Problem and Extremal Problems*, *Translations of Mathematical Monographs* No. 50 (Amer. Math. Soc., Providence, RI, 1977).
[65]I. M. Tkachenko, Y. V. Arkhipov, and A. Askaruly, *The Method of Moments and Its Applications in Plasma Physics* (Lambert, 2012).
[66]D. Varentsov, I. M. Tkachenko, and D. H. H. Hoffmann, Phys. Rev. E **71**, 066501 (2005).
[67]I. M. Tkachenko, "*Sum rules and exact relations for quantal coulomb systems*," *International Conference on Operator Theory and Its Applications in Mathematical Physics* (Stefan Banach International Mathematical Center, Będlewo, Poland, 2002), Book of Abstracts, p. 20.
[68]R. P. Feynman, Phys. Rev. **94**, 262 (1954).
[69]R. Nevanlinna, "Asymptotische Entwicklungen beschrä nkter Funktionen und das Stieltjessche Momentenproblem," in *Suomalaisen Tiedeakatemian Kustantama* (Helsinki, 1922), pp. 1–53; J. Shohat and J. Tamarkin, *The Problem of Moments* (American Mathematical Society, New York, 1943).
[70]N. I. Akhiezer, *The Classical Moment Problem* (Hafner Publishing Company, New York, 1965).
[71]Y. V. Arkhipov, A. Askaruly, D. Ballester, A. E. Davletov, I. M. Tkachenko, and G. Zwicknagel, Phys. Rev. E **81**, 026402 (2010).
[72]S. V. Adamjan, I. M. Tkachenko, J. L. Muñoz-Cobo González, and G. Verdú Martín, "Supplemental material," Phys. Rev. E **48**, 2067 (1993). see also Sec. 2.3.
[73]I. M. Tkachenko, P. Fernández de Córdoba, and M. Urrea, J. Phys. A **29**, 2599 (1996).
[74]J.-L. Bretonnet and A. Derouiche, Phys. Rev. B **38**, 9255 (1988).
[75]F. J. Rogers, D. A. Young, H. E. DeWitt, and M. Ross, Phys. Rev. A **28**, 2990 (1983).
[76]D. A. Young, E. M. Corey, and H. E. DeWitt, Phys. Rev. A **44**, 6508 (1991).
[77]S. Chiesa, D. M. Ceperley, R. M. Martin, and M. Holzmann, Phys. Rev. Lett. **97**, 076404 (2006).
[78]H. Yasuhara, Solid State Commun. **11**, 1481 (1972).
[79]V. M. Adamyan and I. M. Tkachenko, "Solution of the truncated matrix Hamburger moment problem according to M. G. Krein," in *Proceedings of the Mark Krein International Conference on Operator Theory and Applications, Volume II, Operator Theory and Related Topics* (Birkhäuser, Basel, 2000), Vol. 118, pp. 33–52.
[80]H. Reinholz, R. Redmer, G. Röpke, and A. Wierling, Phys. Rev. E **62**, 5648 (2000).
[81]H. Reinholz, G. Röpke, S. Rosmej, and R. Redmer, Phys. Rev. E **91**, 043105 (2015).
[82]M. Veysman, G. Röpke, M. Winkel, and H. Reinholz, Phys. Rev. E **94**, 013203 (2016).
[83]M. Veysman, G. Röpke, and H. Reinholz, Phys. Plasmas **28**, 103303 (2021) and references therein.
[84]G. Röpke, R. Redmer, and A. Wierling, Phys. Plasmas **7**, 39 (2000) and references therein.